

Full-hierarchy Quiver Theories of Electroweak Symmetry Breaking and Fermion Masses

Gustavo Burdman^a Nayara Fonseca^a Leonardo de Lima^a

^a*Instituto de Física, Universidade de São Paulo,
R. do Matão 187, São Paulo, SP 05508-900, Brazil*

E-mail: burdman@if.usp.br, nayara.focs@gmail.com,
leonardodelima@gmail.com

ABSTRACT: We consider quiver theories in four dimensions with a large ultra-violet cut-off. These theories require that an ordered set of vacuum expectation values for the link fields develops dynamically and can be obtained from the coarse deconstruction of extra-dimensional theories in an AdS background. These full-hierarchy quiver theories form a large class which include AdS₅ models as a limit, but which have a distinctive phenomenology. As an example, in this paper we show that fermions can be introduced in a way that can at the same time generate the fermion mass hierarchy and have flavor violation consistent with experimental bounds, when the mass scale of the color-octet gauge excitation is above 3 TeV. We also show that electroweak precision constraints are satisfied by this mass scale, without the need to extend the gauge sector to protect against custodial violation.

KEYWORDS: electroweak symmetry breaking; fermion masses; flavor violation

Contents

1	Introduction	1
2	Full-hierarchy Quiver Theories	4
3	Fermion Localization in Quiver Space	5
4	Mass Hierarchies and Flavor Violation	8
4.1	Localization and Flavor Violation	9
4.2	Flavor Violation Bounds	12
5	Electroweak Precision Constraints	17
6	Conclusions and Outlook	19

1 Introduction

Despite the continued experimental success [1] of the standard model (SM), several fundamental questions remain unanswered in particle physics. Among these are the origin of electroweak symmetry breaking and fermions masses. In the SM, the Higgs sector is composed of a scalar doublet, which results in gauge bosons and fermion masses as it acquires a vacuum expectation value (VEV). This symmetry breaking sector of the SM leaves a remnant state, the Higgs boson, which may have been recently observed at the LHC [2]. More importantly, even if the Higgs boson is observed it remains unclear what keeps the weak scale –in the SM determined by the scale at which the Higgs VEV develops– from running away to the cutoff of the theory, presumably a much higher ultra-violet (UV) scale such as the Planck mass, M_P . The problem of keeping the weak scale separated from the UV cutoff in a theory with an elementary Higgs boson is what we call the hierarchy problem.

It is possible to protect the Higgs mass from the quadratic divergences that would drive it and the weak scale to the UV cutoff by making use of symmetries. Such is the case with weak-scale supersymmetric models [3]. However, the origin of the supersymmetry breaking scale leading to the now stable weak scale, becomes the new unknown. In addition, the generation of fermion masses poses a problem typically leading to large flavor violation and CP asymmetries. Alternatively, it is possible to naturally generate a large weak-scale/UV-scale hierarchy by assuming a new asymptotically-free interaction getting strong at the TeV scale, such as in Technicolor theories [4]. These scenarios also have a problem with large flavor violation since in order to accommodate fermion masses the interaction has to be embedded in extended gauge sectors. Furthermore, the need to add new chiral

fermions has an unavoidable impact in electroweak precision constraints, particularly the S parameter.

More recently, a way of solving the hierarchy problem by using a curved extra dimension in an anti-de Sitter (AdS) background has been formulated [5–7]. The underlying assumption in AdS₅ theories is that they are in some way dual to 4D strongly coupled sectors near conformality, such as walking technicolor (WTC) [4]. Much like in 4D strongly coupled theories, these models tend to have a large S parameter, which can however be controlled by moderately increasing the Kaluza-Klein (KK) mass scale. Initially, it appeared that the fermion mass hierarchy could be naturally explained by the localization of the fermion zero-modes in the extra dimension, controlled by parameters of order one [6, 7], all while not incurring in too large tree-level flavor violation. However, the flavor-violating contributions of KK gluons to kaon observables pushes (in the most generic scenario) the KK mass scale up to a few tens of TeV, resulting in considerable fine-tuning [8]. Thus, these 5D constructions expected to be dual to 4D strongly coupled sectors, present problems similar to the ones plaguing the original TC-ETC models.

In this paper we present a set of theories that are designed to generate a large hierarchy between the weak scale and a large UV scale. These purely four-dimensional models consist of gauge groups joined by sigma models, the so-called quiver theories, and they are cousins of AdS₅ theories in that they are related to them by the procedure called deconstruction [9]. They are characterized by highly ordered vacuum expectation values (VEVs) of the sigma models, starting just below the desired UV scale and going all the way to the weak scale. The limit of large number of gauge groups and large value of the UV VEV, corresponds to recovering AdS₅ theories and we will call it the continuum limit. However, the four-dimensional quiver theories can be quite different from AdS₅, particularly when we consider the opposite limit, which we can call coarse discretization, and that corresponds to using only a few gauge groups. Thus, we are interested in working far from the continuum limit to build our models, so that these quiver theories cannot have an interpretation as a low-energy AdS₅ model that can be obtained by truncating the Kaluza-Klein towers [10]. As we will show below, the result of a coarse discretization is very different from this procedure since, for instance, it gives very different couplings of the excited states to zero-mode fermions, resulting in a distinct phenomenology. We will show that quiver theories with few gauge groups or “sites” can generate a large hierarchy of scales, as well as the fermion mass hierarchy just as AdS₅ models, while not generating too large flavor violation. This particular advantage, together with the fact that these theories are fundamentally different from the warped extra dimension models, makes a full exploration of full-hierarchy quiver theories an interesting proposition.

At a more fundamental level, we see that AdS₅ theories are only a small fraction of a much larger set of theories capable of generating large hierarchies. Formulating these vast set of theories, what we call Full-hierarchy Quiver Theories (FHQT), with AdS₅ as a limiting case for large number of groups, allows us to generalize the good features of AdS₅ theories to their coarse FHQT cousins. Since these are quantitatively different from AdS₅ we expect important phenomenological distinctions between them and FHQT models with a sufficiently small number of sites. In order to start studying these differences, we will

build coarse quiver theories very similar to bulk AdS₅ models and explicitly show that they can have potentially much less flavor violation than them. Here we will consider models that in the continuum limit would result in an infrared (IR) localized Higgs. However, it is possible to obtain a dynamical Higgs in FHQT very much in the same way that composite Higgs models emerge in AdS₅. We leave this to a separate companion publication [11]. In general, it is possible to reproduce any model in the AdS₅ limit of FHQT, so we could study it in the coarse limit. Thus, besides the issue of flavor violation with a localized Higgs, or reproducing Gauge-Higgs unification in a coarse theory, we can consider various other issues in this general framework. For instance, issues from how the conformal behavior of the AdS₅ theories manifests itself in the quiver theories, to the existence of a strongly coupled “dual” which the four-dimensional quiver theories correspond to, should be addressed in the future. For now, we will concentrate on the phenomenological aspects related to model building the mechanism for electroweak symmetry breaking (EWSB) and fermion masses. But more theoretical ramifications may and should be addressed concerning the use of FHQT and their behavior as quantum field theories.

The models will have a stabilized gauge hierarchy and a natural origin for the fermion hierarchy. Just as in warped extra dimensions, the origin of the fermion mass hierarchy is *a priori* independent of the stabilization of the Higgs sector. The gauge hierarchy problem is solved as long as the Higgs is IR-localized. IR localization of the Higgs can be achieved through specific mechanisms. For the purpose of this paper we assume it will be fully localized in the so called IR site, which in the continuum limit would correspond to localizing the Higgs in the IR brane. Dynamical Higgs localization is left for a separate work [11], and can be achieved in a way very similar to composite models [12] in the continuum limit. In this setup, we will consider flavor by introducing fermion localization in theory space, and will study the resulting flavor violation phenomenology in coarse FHQT. We will show that in these cases it is possible to have very little flavor violation, unlike in the continuum limit. We will also consider the electroweak bounds on coarse FHQT. In the AdS₅ case, these impose an extension in the electroweak gauge sector due to the presence of large isospin violation. We will show that in general FHQT do not need custodial protection to have sufficiently small contributions to the T parameter.

There are several papers in the literature making use of deconstruction techniques to obtain models of electroweak symmetry breaking and/or flavor. For instance, in Ref. [13] a 3-site Higgsless model is proposed, and its flavor structure studied in [14]. In Ref. [15] the flavor physics of composite Higgs models like those of [12] is explored using a 2-site setup with flavor symmetries. In Ref. [16] the Higgs sector of this setup is considered, whereas 2 and 3-site models with custodial protection are considered in Ref. [17]. A more general approach to a 4D pNGB Higgs is presented in Ref. [18], although it is still tied to the coset $SO(5)/SO(4)$ presented in [12]. In our work we considered a larger number of sites in order to explore the feasibility of the non-hierarchical primordial Yukawa couplings. In doing so, we will see that our results, if viewed from a 2-site model perspective, encode the resulting effective flavor symmetries of the fully-deconstructed AdS₅ theory. In addition, we will see that it is not necessary to consider custodial protection in the gauge sector of the model in order to avoid too large a tree-level contribution to the T parameter. As a result, the

minimal composite Higgs model will have a smaller symmetry than in the papers above. Then the FHQT constructions bring a new perspective to both the flavor and electroweak sectors.

The rest of the paper is organized as follows: in Section 2 we present the FHQT and their relation to a coarse deconstruction of AdS₅ models. In Section 3 we show how fermions are included and how the fermion mass hierarchy can be obtained naturally. We study flavor violation in Section 4, where we show that it is possible to obtain small enough violation to accommodate all experimental bounds, while keeping the new physics mass scale close to the TeV. The electroweak precision bounds are considered in 5. We finally conclude in Section 6.

2 Full-hierarchy Quiver Theories

In this section we describe the basics of FHQT. As an example let us consider the product gauge group $G_0 \times G_1 \times \dots \times G_j \times G_{j+1} \dots \times G_N$. In addition, we have a set of scalar link fields Φ_j , with $j = 1$ to N , transforming as bi-fundamentals under $G_{j-1} \times G_j$. The action for the theory is

$$S = \int d^4x \left\{ - \sum_{j=0}^N \frac{1}{2g_j^2} \text{Tr} \left[F_{\mu\nu}^{(j)} F^{\mu\nu(j)} \right] + \sum_{j=1}^N \text{Tr} \left[(D_\mu \Phi_j)^\dagger D^\mu \Phi_j \right] - V(\Phi_j) + \dots \right\} \quad (2.1)$$

where the traces are over the groups' generators, and the dots at the end correspond to terms involving fermions and will be discussed in the next section. We assume that the potentials for the link fields give them a vacuum expectation value (VEV) which breaks $G_{j-1} \times G_j$ down to the diagonal group, and result in non-linear sigma models for the Φ 's

$$\Phi_j = \frac{v_j}{\sqrt{2}} e^{i\sqrt{2}\pi_j^a \hat{t}^a / v_j} , \quad (2.2)$$

where the \hat{t}^a 's are the broken generators, the π_j^a the Nambu-Goldstone Bosons (NGB); and v_j are the VEVs of the link fields. We will consider here the situation where the VEVs are ordered in such a way that $v_1 \dots > v_j \dots > v_N$. We parametrize the ordering by defining the VEVs as

$$v_j \equiv v q^j , \quad (2.3)$$

where $0 < q < 1$ is a dimensionless constant, and v is a UV mass scale that can be regarded as the UV cutoff. We will also assume that all the gauge groups are identical and that their gauge couplings satisfy

$$g_0(v) = g_1(v_1) = \dots = g_j(v_j) = g_{j+1}(v_{j+1}) = \dots \equiv g . \quad (2.4)$$

The model can be illustrated by the quiver diagram of Figure 1.

This purely 4D theory can be obtained from deconstructing an extra-dimensional theory in an AdS₅ background [19–21]. Discretizing a 5D gauge theory in an AdS₅ background

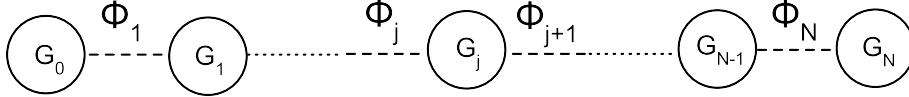


Figure 1. Quiver diagram for the theory described by (2.1)..

by a discrete interval $1/gv$ in N intervals results in the action (2.1), with the appropriate identification of the 5D gauge coupling, plus the matching

$$q \leftrightarrow e^{-k/gv} . \quad (2.5)$$

However, in order for the 4D theory defined by (2.1) to remain a good description of the continuum 5D theory, the AdS_5 curvature should satisfy $k < v$, or q close to 1. When this is satisfied, getting closer to the continuum limit by increasing the number of sites N guarantees an increasing similarity with the 5D theory [21]. For instance, generating the hierarchy between the Planck and the weak scales while satisfying $k < v$ requires typically that $N > 35$, which results in a low energy theory very close to the continuum one. Under these conditions, 4D theories with $k < v$ are just discrete descriptions of the AdS_5 theory.

On the other hand, if we consider (2.1) as just a 4D theory, we are free to make use of values of q far from what would constitute the continuum 5D limit, i.e. $q \ll 1$. In these theories it will be possible to obtain a large hierarchy of scales with smaller values of N , as low as just a few. For instance, if $v \lesssim M_P$ and $v_N \simeq O(1)$ TeV, then we can write

$$q = 10^{-16/N} . \quad (2.6)$$

For instance, for $N = 4$ we have $q = 10^{-4}$, very far from the continuum limit. The theories resulting in these region of the parameters of the action in (2.1) will have a very different behavior than a mere discretization of AdS_5 . Their spectrum and its properties, such as couplings to SM matter, differ significantly and therefore they merit a detailed study.

There are several aspects of FHQT worth exploring. Regarding their use to build models of EWSB, the most urgent appears to be the modeling of the Higgs sector leading to EWSB, and the generation of fermion masses. We consider the dynamical origin of the Higgs sector in a separate publication [11], where the Higgs is a remnant pseudo-NGB (pNGB). For this paper, we concentrate on the issue of fermion masses and assume a very simple Higgs sector, one that captures the essential features of the Yukawa interactions in these models. Our aim is to explore the consequences of naturally generating the fermion mass hierarchy in FHQT. Specifically, we want to know if is possible to build models with acceptable levels of flavor violation. This is important in light of the great difficulties encountered in AdS_5 models regarding this issue [23]. It is also generally of great interest to explore new models of the fermion hierarchy and their flavor-violating effects.

3 Fermion Localization in Quiver Space

In this section we incorporate fermions to the FHQT. The main goal is to model fermion masses in the context of Higgs sector models that solve the hierarchy problem within the

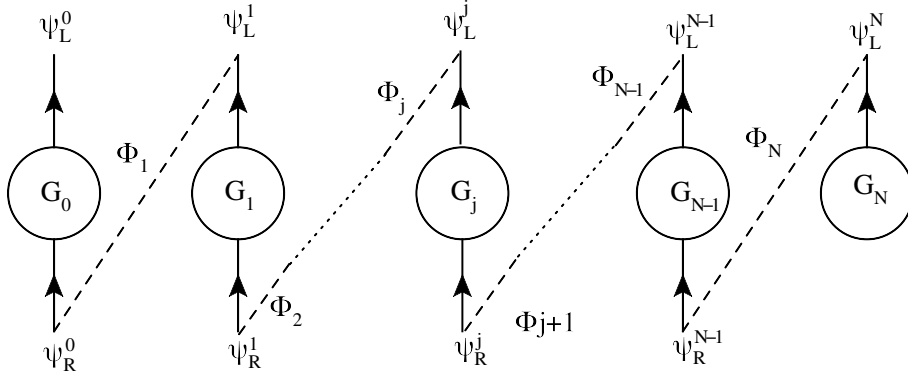


Figure 2. Quiver diagram for the theory described by (3.1), for a spectrum with a left-handed zero mode.

framework of FHQT.

We consider vector-like fermions ψ^j transforming in the fundamental representation of the groups G_j . The action of (2.1) is then enlarged by the fermion action given by

$$S_f = \int d^4x \sum_{j=0}^N \left\{ \bar{\psi}_L^j i \not{D}_j \psi_L^j + \bar{\psi}_R^j i \not{D}_j \psi_R^j - (\mu_j \bar{\psi}_L^j \psi_R^j + \lambda_j \bar{\psi}_R^{j-1} \Phi_j \psi_L^j + \text{h.c.}) \right\}, \quad (3.1)$$

which is represented by the quiver diagram of Figure 2. The vector-like masses μ_j preserve the gauge symmetries. The Yukawa term is invariant since the links transform as $\Phi_j \rightarrow g_{j-1} \Phi_j g_j^\dagger$. The Yukawa couplings are allowed to be site-dependent, which is the most general situation in the 4D theory. If one wanted to match to the continuum limit of the AdS₅ theory we should take them to be universal, as shown in Ref [22]. In the unitary gauge we make the replacement $\Phi_j \rightarrow v_j/\sqrt{2}$, which leads to a non-diagonal mass matrix for the fermions. We diagonalize to the mass eigenstate basis through the unitary transformations

$$\psi_{L,R}^j = \sum_{n=0}^N h_{L,R}^{j,n} \chi_{L,R}^{(n)}, \quad (3.2)$$

where the $\chi_{L,R}^{(n)}$ are the mass eigenstates. Imposing the equations of motion, results in the elements of the rotation matrices satisfying the equations [22]

$$\left(\mu_j^2 + \frac{\lambda_j^2 v_j^2}{2} - m_n^2 \right) h_L^{j,n} - \frac{\lambda_j v_j}{\sqrt{2}} \mu_{j-1} h_L^{j-1,n} - \frac{\lambda_{j+1} v_{j+1}}{\sqrt{2}} \mu_j h_L^{j+1,n} = 0 \quad (3.3)$$

$$\left(\mu_j^2 + \frac{\lambda_{j+1}^2 v_{j+1}^2}{2} - m_n^2 \right) h_R^{j,n} - \frac{\lambda_j v_j}{\sqrt{2}} \mu_j h_R^{j-1,n} - \frac{\lambda_{j+1} v_{j+1}}{\sqrt{2}} \mu_{j+1} h_R^{j+1,n} = 0 \quad (3.4)$$

where m_n is the mass of the mass eigenstate $\chi_{L,R}^{(n)}$. The solutions of these equations can be obtained [21] and in the continuum limit would match to the solutions for the wavefunctions of the Kaluza-Klein fermions in the AdS₅ [22]. But here we stay far from the continuum.

We are interested in studying the fermion zero-modes. These satisfy the simple equations of motion

$$\mu_j h_L^{j,0} + \frac{\lambda_{j+1}}{\sqrt{2}} v_{j+1} h_L^{j+1,0} = 0 , \quad (3.5)$$

for the left-handed zero mode, and

$$\mu_j h_R^{j,0} + \frac{\lambda_j}{\sqrt{2}} v_j h_R^{j-1,0} = 0 , \quad (3.6)$$

for the right-handed zero mode. We can define the localization parameter ν_L for the left-handed zero mode by

$$\sqrt{2} \frac{\mu_j}{v \lambda_{j+1}} \equiv -q^{j+1+\nu_L} , \quad (3.7)$$

and then consistently identify the localization parameter ν_R for a right-handed zero mode by

$$\sqrt{2} \frac{\mu_j}{v \lambda_j} = -q^{j+1+\nu_R} , \quad (3.8)$$

Then, we can see that

$$\frac{h_L^{j+1,0}}{h_L^{j,0}} = q^{\nu_L} , \quad \frac{h_R^{j,0}}{h_R^{j-1,0}} = q^{-(1+\nu_R)} . \quad (3.9)$$

Thus, we have traded the ratio of vector masses to Yukawa couplings for a parameter (ν_L or ν_R) that will determine how much of each fermion in the quiver diagram the zero-mode fermion contains. We can then write

$$h_{L,R}^{j,0} = z_{L,R}^j h_{L,R}^{0,0} , \quad (3.10)$$

where we have defined

$$z_L \equiv q^{\nu_L} , \quad z_R \equiv q^{-(1+\nu_R)} . \quad (3.11)$$

On the other hand, the normalization conditions require that

$$\sum_{j=0}^N |h_{L,R}^{j,0}|^2 = 1 , \quad (3.12)$$

which we use to obtain

$$h_{L,R}^{0,0} = \sqrt{\frac{1 - z_{L,R}^2}{1 - z_{L,R}^{2(N+1)}}} , \quad (3.13)$$

We can use these results to compute the couplings of the fermion zero mode to various states. Here we will consider first the Yukawa couplings to the Higgs. As it is shown in Ref. [11], in order to solve the hierarchy problem, the Higgs must be coupled mostly to the gauge groups that survive at lower energies, particularly G_N . This is the analog of having a Higgs localized close to the IR brane in AdS₅ models in 5D. For simplicity we will assume that the Higgs only transforms under G_N (“localized” at the end of the quiver). In Ref. [11] we show dynamical mechanisms to do just that. Here we are interested in

the Yukawa couplings and their general behavior. With such a “N-Localized” Higgs, the Yukawa coupling of a given zero-mode fermion is defined by

$$\mathcal{L} = -\mathcal{Y}\bar{\psi}_L^N H\psi_R^N + h.c. = -\mathcal{Y}h_L^{*N,0}h_R^{N,0}\bar{\chi}_L^{(0)}H\chi_R^{(0)} + h.c. , \quad (3.14)$$

where the primordial Yukawa \mathcal{Y} is assumed to be an $O(1)$ number. The resulting effective Yukawa coupling of the fermion zero-mode is

$$Y = \mathcal{Y}z_L^N z_R^N h_L^{0,0} h_R^{0,0} . \quad (3.15)$$

Thus, we see that zero-mode fermions with large components of their eigenstate wave-functions coming from $\psi_{L,R}^i$ with i close or equal to N , will have unsuppressed Yukawa couplings with the “N-localized” Higgs. On the other hand, zero-mode fermions with wave-functions built mostly of $\psi_{L,R}^i$ with i closer to 0 will have largely suppressed Yukawa couplings in (3.15). We can then build theories of flavor by choosing the quiver-diagram localization of the zero-mode fermion, much in the same way it is done in AdS₅ theories. Fermion-mass hierarchies can be built by appropriately choosing the localization parameters for the fermions in the quiver theory, ν_L and ν_R for each generation. This can be achieved with quiver theories with a small number of sites, such as 4 or 5, very far from the continuum limit.

One potential worry is the presence of flavor changing neutral currents (FCNCs) at tree level, induced by the non-universal couplings of massive gauge bosons to the zero-mode fermions that necessarily appear as a consequence of the different localization in the quiver diagram. In fact, these FCNCs are a very important problem in AdS₅ theories and result in the most stringent of bounds [8]. In the next section, we address this issue in FHQT and show that in them it is possible to build the SM fermion mass hierarchy without large FCNCs at tree level. In particular, we show that is possible to find solutions where FCNCs are nearly absent in the down-type quark sector, which is typically the most binding.

4 Mass Hierarchies and Flavor Violation

In order to study flavor violation in FHQT, we first need to compute the couplings of massive gauge bosons to zero-mode fermions. We first notice that the wave-function of a zero-mode fermion can be written as

$$\chi_{L,R}^{(0)} = \sum_{j=0}^N h_{L,R}^{*j,0} \psi_{L,R}^j , \quad (4.1)$$

in terms of the quiver fermions. Likewise, and assuming a generic gauge group in the sites of the quiver diagram, the mass-eigenstates of the gauge bosons can be written in terms of the quiver gauge bosons as

$$A_\mu^{(n)} = \sum_{j=0}^N f_{j,n}^* A_\mu^j , \quad (4.2)$$

with $f_{j,n}$ the coefficient linking the gauge boson in site j with the mass-eigenstate n in the rotation to mass eigenstates. We are interested in obtaining the coupling of the $n = 1$ to

the zero-mode fermions since this state gives the largest FCNCs effect. We can compute this coupling

$$g_{L,R}^{01} \bar{\chi}_{L,R}^{(0)} \gamma^\mu A_\mu^{(1)} \chi_{L,R}^{(0)}, \quad (4.3)$$

where we assumed that group generators are absorbed in the definition of the gauge fields, and we obtain

$$g_{L,R}^{01} = \sum_{j=0}^N g_j \left| h_{L,R}^{j,0} \right|^2 f_{j,1}, \quad (4.4)$$

where g_j are the gauge couplings associated to the group G_j in the quiver. As mentioned above, we will assume $g_j = g$ for all j . To be more precise, we actually mean to say that $g_j = g(\nu_j)$, with $g(\mu)$ the same *running* coupling for all gauge groups in the quiver.

For fixed values of N the coefficients $f_{j,1}$ can be obtained by diagonalizing the gauge boson mass matrix [21, 22]. Then, we can obtain the coupling of zero-mode fermions to the first excited state of the gauge bosons, normalized by the gauge coupling g . These couplings are of great interest for various reasons. For instance, the s-channel production of the first-excited states of the gauge bosons is determined by them, so they would play a central role in the collider searches for these theories. But they could also lead to tree-level flavor violation since their couplings to the SM fermions are generally not universal. The couplings in (4.4) depend on the localization parameters ν_L and ν_R , which are to be chosen appropriately to get the correct zero-mode masses as well as mixings, as mentioned in the previous section.

4.1 Localization and Flavor Violation

Here we consider the coupling of the zero-mode fermions to the first excited state of a gluon. In Figure 3 we show the coupling of a left-handed zero-mode fermion as a function of the localization parameter redefined as $c_L \equiv \nu_L + 1/2$, and for various values of the number of sites in the quiver, N . We can see that as N increases from small values, corresponding to coarse discretization, to large values nearing the continuum limit, the coupling goes to its continuum limit, as it can be verified by comparing the $N = 90$ case with the results in Ref. [7]. We can see then that these couplings of great phenomenological importance are quite different far from the continuum. The same can be done for the right-handed couplings.

As an example, we study these couplings for the $N = 4$ case, i.e five sites. We compute the coupling of zero-mode fermions to the first gauge excitation as a function of the localization parameter for the zero-mode fermion, $\nu_{L,R}$. The case of a left-handed zero mode fermion is shown in the solid line in Figure 4. We observe that there are two plateaus: one above $c_L > 1/2$, the other for $c_L < 0.25$. The transition region is rather small. Thus, a given solution for the c_L 's (i.e. for the zero-mode fermion masses and mixings) such that they are on either plateau, will have effectively very small or negligible tree-level flavor violation. We can do the same for the right-handed down and up zero-mode fermions. The corresponding couplings to the first-excited gauge boson state are plotted in the solid lines of Figures 5 and 6.

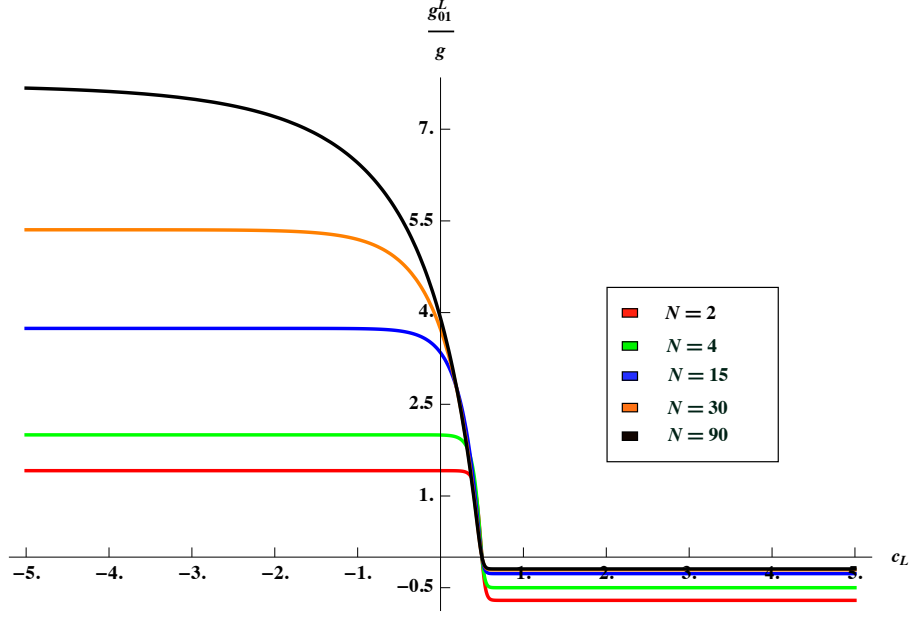


Figure 3. Couplings of a left-handed zero-mode fermion to the first excited state of a gauge boson, normalized to the zero-mode gauge boson coupling, as a function of the localization parameter c_L . For the left side of the plot and starting from the bottom: $N = 2$, $N = 4$, $N = 15$, $N = 30$ and $N = 90$.

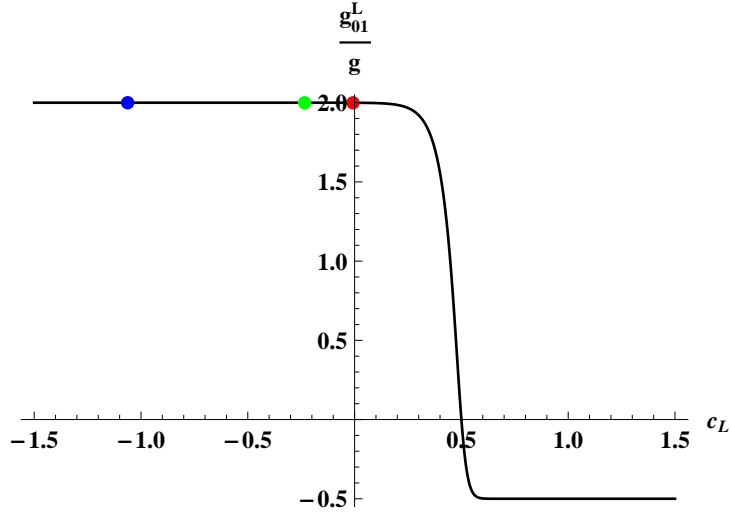


Figure 4. Couplings of the left-handed zero-mode quarks to the first excited state of the gauge boson, in units of the zero-mode gauge coupling, vs. the localization parameter c_L defined in the text (solid line). The dots correspond to the localization of the solution called **case A**.

Thus, we want to find solutions for the localization parameters $c_{L,R}^i$'s, where the $i = 1, 2, 3$ denotes generation, which lay mostly on the plateaus in order to minimize flavor violation. We will show two such examples. In the first case, **case A**, we minimize the

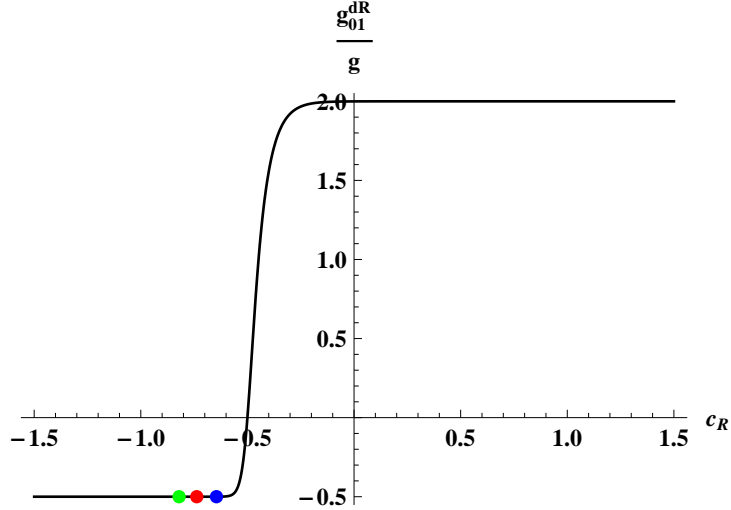


Figure 5. Couplings of the right-handed zero-mode down quarks to the first excited state of the gauge boson, in units of the zero-mode gauge coupling, vs. the localization parameter c_R defined in the text (solid line). The dots correspond to the localization of the solution called **case A**.

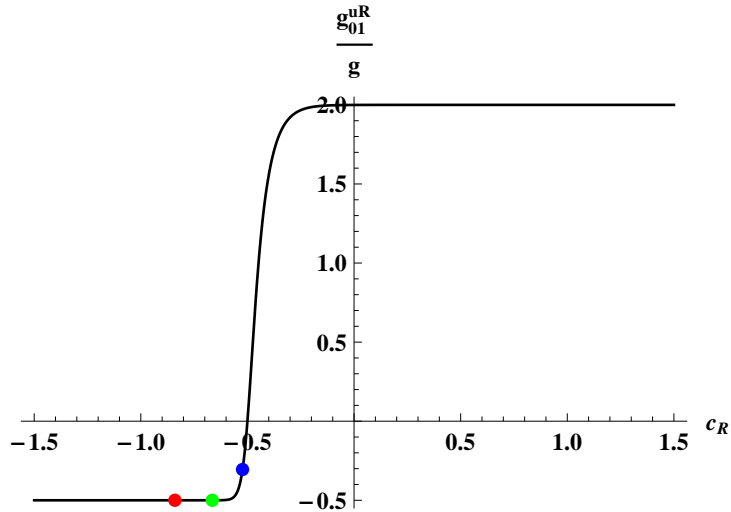


Figure 6. Couplings of the right-handed zero mode up quarks to the first excited state of the gauge boson, in units of the zero-mode gauge coupling, vs. the localization parameter c_R defined in the text (solid line). The dots correspond to the localization of the solution called **case A**.

amount of flavor violation necessary to obtain the correct masses and mixings in the quark sector. This is achieved by localizing the right-handed sector as close to the UV plateau as possible, while the left-handed quark sector is localized towards the IR plateau. In the second case, **case B**, the right-handed down sector remains in the UV plateau, whereas the left-handed sector and most of the right-handed up sector is also there, but with small amounts of flavor violation.

Case A: In Figure 4, we plot the coupling of the first excited state of a gauge boson (normalized to its zero-mode coupling) as a function of the localization parameters in the quiver diagram. The dots show a solution for the quark sector, that results in the correct masses and mixings. In this case, the left-handed quarks are localized in the IR plateau. Although their localizations in the quiver imply different Yukawa couplings, they will have nearly universal couplings to the first excited state of the gauge bosons, resulting in very little or no tree-level flavor violation. The solution for the localization coefficients $c_{L,R}^i$ are color coded. We see in Figure 4 that the couplings of the left-handed doublet zero mode quark to the first gauge excitation are universal, so they will not result in tree-level flavor violation. The same can be concluded by observing the couplings of the down-type right handed zero-mode quarks, Figure 5. Thus, we see that this solution of the $N = 4$ example *does not result in tree-level flavor violation in the down-quark sector*. This should be compared with the situation in RS models in an AdS₅ background, where flavor violation at tree level is unavoidable in the down sector, leading to very stringent bounds on the scale of the gauge excitations [23]. Finally, the right-handed up-sector couplings to the first gauge boson excitation are shown in Figure 6. We see that it is not possible to have universal couplings as in the right-handed down sector. This is due to the need for the right-handed top to be closer to the IR in order to obtain the correct top quark mass. This will lead to the leading source of tree-level flavor violation in this case, which will be in the up sector in observables such as $D^0\bar{D}^0$ mixing. In the next subsection we show that this effect is very small and quite compatible with experiment.

As we increase N , the curves in Figures 4, 5 and 6 will tend to their analogous in the continuum AdS₅ limit [7]. Thus, we see that, although FHQT share some of the features of AdS₅ models, they behave in a different way when it comes to the amount of flavor violation induced. This difference is one of the key points that make FHQT more viable phenomenologically than models based on warped extra dimensions.

Case B This case is a small variation of the previous one: the difference is that now the left-handed quarks are localized towards the UV of the quiver. The right-handed down sector would remain also in the UV, with the right-handed up sector in the UV with one exception due to the need for a large top quark mass. This new solution is shown in Figures 7, 8 and 9. We see that the right-handed down sector remains universally coupled to the gauge excitations, whereas now not only there is flavor violation in the right-handed up sector but also in the left-handed sector, as shown in Figure 7. This results in slightly larger flavor violation in the down sector, but still not as large as the effect in the continuum limit. In what follows we evaluate the amount of flavor violation incurred in each case. We will see that in both cases flavor violation bounds can be satisfied. On the other hand, the difference between cases **A** and **B** will be more relevant when computing electroweak precision constraints. This will be done in the next section.

4.2 Flavor Violation Bounds

In order to study the effects of flavor violation we need to obtain the tree-level couplings of fermions to the first-excited gauge boson. Here we concentrate in quark couplings since

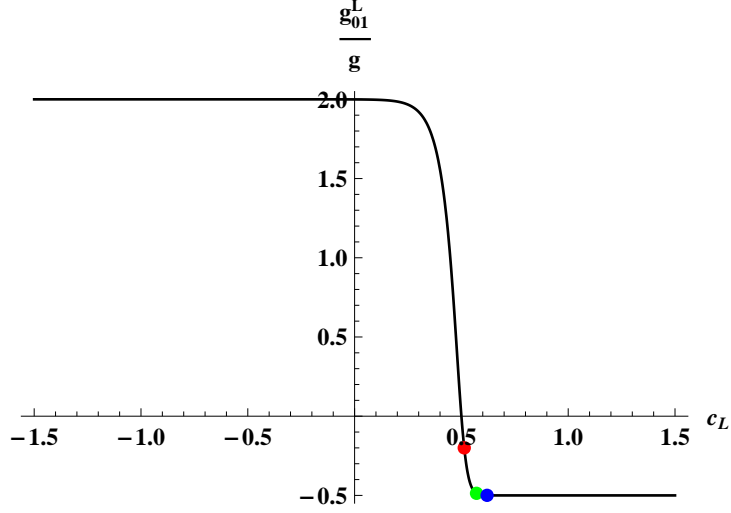


Figure 7. Couplings of the left-handed zero-mode quarks to the first excited state of the gauge boson, in units of the zero-mode gauge coupling, vs. the localization parameter c_L defined in the text (solid line). The dots correspond to the localization of the solution called **case B**.

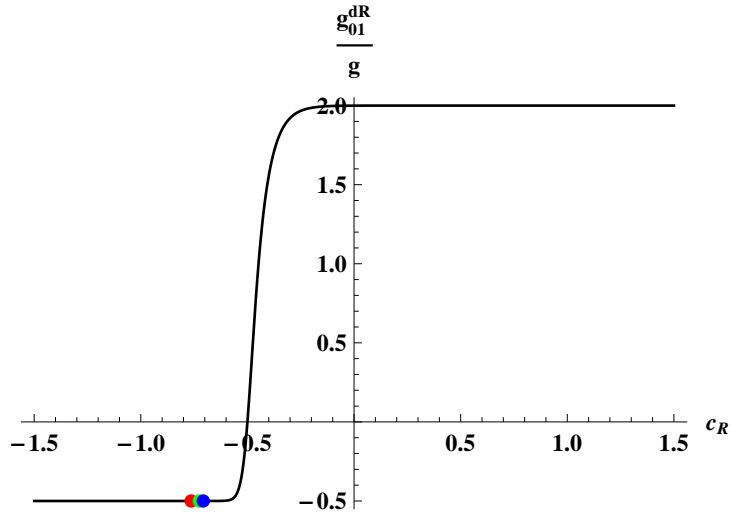


Figure 8. Couplings of the right-handed zero-mode down quarks to the first excited state of the gauge boson, in units of the zero-mode gauge coupling, vs. the localization parameter c_R defined in the text (solid line). The dots correspond to the localization of the solution called **case B**.

they are the most constraining. In both examples, cases **A** and **B**, Figures (4-9) give the couplings of quarks to the first gauge excitation in the interaction (diagonal) basis. To obtain the flavor-violating interaction, we must rotate to the mass basis. For instance, if we define the couplings of the left-handed up-type quarks in the mass eigen-basis as given

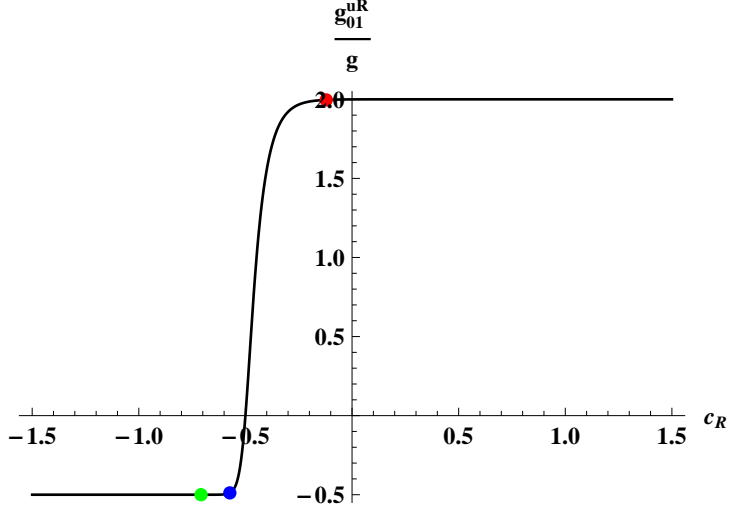


Figure 9. Couplings of the right-handed zero-mode up quarks to the first excited state of the gauge boson, in units of the zero-mode gauge coupling, vs. the localization parameter c_R defined in the text (solid line). The dots correspond to the localization of the solution called **case B**.

by

$$G_L^U \equiv U_L^{-1} \begin{pmatrix} g_{u_L} & 0 & 0 \\ 0 & g_{c_L} & 0 \\ 0 & 0 & g_{t_L} \end{pmatrix} U_L ,$$

where U_L is a unitary matrix that rotates to the mass eigenstates, the couplings g_{u_L} , g_{c_L} and g_{t_L} are the one given by the dots in Figures 4 and 7 for cases **A** and **B**, respectively. The non-diagonal coupling matrix G_L^U contains the flavor violating couplings. There will be an analogous definition for the right-handed up sector in terms of U_R , as well as for the down sector, both left- and right-handed. The tree-level flavor violation induced by the non-diagonal entries in the G 's will result in bounds on the mass of the first excitation of the gauge bosons in FHQT. In order to be conservative, we will consider the effects of the first excitation of the gluon, that is we assume that $SU(3)_c$ propagates in the quiver diagram. Although this is not necessary in these theories, it will provide the most stringent bound and will allow us to compare with the analogous flavor-violation bounds in AdS_5 , the continuum limit.

The effective Hamiltonian for $\Delta F = 2$ transitions will receive the following contributions when the excited gluon is integrated out

$$H_{\text{eff.}} = \frac{1}{M_G^2} \left[\frac{1}{6} G_L^{ij} G_L^{ij} (\bar{q}_L^{i\alpha} \gamma^\mu q_{L\alpha}^j) (\bar{q}_L^{i\beta} \gamma^\mu q_{L\beta}^j) + (\text{L} \leftrightarrow \text{R}) \right. \\ \left. - G_L^{ij} G_R^{ij} \left((\bar{q}_R^{i\alpha} q_{L\alpha}^j) (\bar{q}_L^{i\beta} q_{R\beta}^j) - \frac{1}{3} (\bar{q}_R^{i\alpha} q_{L\beta}^j) (\bar{q}_L^{i\alpha} q_{R\beta}^j) \right) \right] \quad (4.5)$$

This can be matched with the low energy $\Delta F = 2$ Hamiltonian, resulting in contributions to some of its Wilson coefficients. Following Ref. [24], the contributions from (4.5) result

in

$$C_M^1(M_G) = \frac{1}{6} \frac{(G_L^{ij})^2}{M_G^2}, \quad C_M^4(M_G) = \frac{G_L^{ij} G_R^{ij}}{M_G^2}, \quad C_M^5(M_G) = \frac{G_L^{ij} G_R^{ij}}{3M_G^2} \quad (4.6)$$

where $M = K, D, B_d, B_s$ refers to the particular meson. The Wilson coefficients are then bound by the fits to flavor data by the UTFit collaboration [24], which provides the most comprehensive treatment of flavor data to bound new physics. The bounds on these coefficients from their latest fit of $\Delta F = 2$ observables is shown in the second column of Table 3. The bounds from kaon physics were updated in Ref. [25]. The third column gives the bounds on the scale of new physics implied by assuming that the Wilson coefficients at Λ are unity. In our case, the Wilson coefficients given in (4.6) have a large suppression and therefore allow for a much lower energy scale M_G . Finally, given that the bounds are obtained at larger scales Λ , in some cases where this scale is considerably larger than M_G , we must correct for the renormalization group evolution that is implied in the bounds.

We first study the bounds on **case A**, presented in the previous subsection and defined in Figures 4 to 6. This case is clearly designed to minimize tree-level flavor violation effects. The choice of localization for quarks in the quiver, defined by the values of the various $c_{L,R}^i$ coefficients and consistent with the physical masses and with the observed V_{CKM} , also fixes the non-diagonal couplings of the mass-basis quarks to the first gauge excitation of the gluon. In Table 1 we show the values of the non-diagonal entries for G_L^U, G_L^D, G_R^U and G_R^D . When comparing (4.6) with the third column of Table 3, we see that for **case A** there are

	L	R		L	R
$ G^{u,c} $	1.1×10^{-5}	2.2×10^{-8}	$ G^{d,s} $	5.7×10^{-5}	1.6×10^{-9}
$ G^{u,t} $	2.0×10^{-4}	2.3×10^{-6}	$ G^{d,b} $	1.9×10^{-4}	2.1×10^{-8}
$ G^{c,t} $	5.5×10^{-6}	6.8×10^{-4}	$ G^{s,b} $	5.9×10^{-5}	2.5×10^{-6}

Table 1. Case A: Non-diagonal values of the quark couplings to the first excitation of the gluon.

virtually no meaningful bounds coming from flavor physics on the mass scale of the first excitations of gauge bosons, even if these are color-octet states. However, as we will see in the next section, the fermion localization in the quiver chosen for **case A**, will result in larger contributions to the S and T parameters.

On the other hand, zero-mode fermion localization in **case B** is chosen so as to minimize effects on electroweak precision observables (see next section). This results in larger flavor-violation effects. The non-diagonal entries of the matrices G_L^U, G_L^D, G_R^U and G_R^D in **case B**, which lead to tree-level flavor violation, are given in Table 2. Comparing these entries with those of Table 1, we see that larger flavor-violating effects are to be expected. These translate into bounds on the mass of the gauge excitation. The bounds from $\Delta F = 2$ operators are shown in the last column of Table 3. The most constraining bound comes from the chirally-enhanced operator O_4 [25]. The bound on $\text{Im}C_K^4$ results in

$$M_G > 3 \text{ TeV} . \quad (4.7)$$

	L	R		L	R
$ G^{u,c} $	2.8×10^{-3}	2.9×10^{-4}	$ G^{d,s} $	5.7×10^{-4}	6.5×10^{-6}
$ G^{u,t} $	4.2×10^{-3}	2.9×10^{-3}	$ G^{d,b} $	5.9×10^{-3}	5.0×10^{-5}
$ G^{c,t} $	3.3×10^{-2}	1.8×10^{-1}	$ G^{s,b} $	6.7×10^{-3}	1.2×10^{-4}

Table 2. Case B: Non-diagonal values of the quark couplings to the first excitation of the gluon.

Another bound from $\Delta S = 2$ physics that is close to this comes from ImC_K^1 , which results in $M_G > 2.6$ TeV. But a limit quite similar to that of (4.7) comes from charm physics. As can be seen in Table 3, the bound on $|C_D^4|$ requires $M_G > 2.9$ TeV. This is due to the fact that the right-handed up sector must be more localized towards the N site in order to get the correct top quark mass. In any case, the bound in (4.7) is just an example of a typical value that would pass all flavor limits in the particular solution shown in Figures 7, 8 and 9. It is not necessarily the smallest possible value for M_G for all solutions. However, it is a good illustration of the fact that in FHQT it is possible to get the fermion mass hierarchy without large flavor violation. This must be contrasted with the typical flavor violation obtained in AdS₅ models, which results in much tighter bounds [8].

Parameter	95% allowed range (GeV ⁻²)	Lower limit on Λ (TeV) for arbitrary NP	Bound on Color-octet Mass in FHQT (TeV)
ReC_K^1	$[-9.6, 9.6] \cdot 10^{-13}$	$1.0 \cdot 10^3$	0.2
ReC_K^4	$[-3.6, 3.6] \cdot 10^{-15}$	$17 \cdot 10^3$	0.1
ReC_K^5	$[-1.0, 1.0] \cdot 10^{-14}$	$10 \cdot 10^3$	0.1
ImC_K^1	$[-2.6, 2.8] \cdot 10^{-15}$	$1.9 \cdot 10^4$	2.6
ImC_K^4	$[-4.1, 3.6] \cdot 10^{-18}$	$49 \cdot 10^4$	3.0
ImC_K^5	$[-1.2, 1.1] \cdot 10^{-17}$	$29 \cdot 10^4$	1.0
$ C_D^1 $	$< 7.2 \cdot 10^{-13}$	$1.2 \cdot 10^3$	1.0
$ C_D^4 $	$< 4.8 \cdot 10^{-14}$	$4.6 \cdot 10^3$	2.9
$ C_D^5 $	$< 4.8 \cdot 10^{-13}$	$1.4 \cdot 10^3$	0.5
$ C_{B_d}^1 $	$< 2.3 \cdot 10^{-11}$	$0.21 \cdot 10^3$	0.3
$ C_{B_d}^4 $	$< 2.1 \cdot 10^{-13}$	$2.2 \cdot 10^3$	0.3
$ C_{B_d}^5 $	$< 6.0 \cdot 10^{-13}$	$1.3 \cdot 10^3$	0.1
$ C_{B_s}^1 $	$< 1.1 \cdot 10^{-9}$	30	0.1
$ C_{B_s}^4 $	$< 1.6 \cdot 10^{-11}$	250	0.1
$ C_{B_s}^5 $	$< 4.5 \cdot 10^{-11}$	150	0.03

Table 3. 95% probability range for $C(\Lambda)$ and the corresponding lower bounds on the NP scale Λ for arbitrary NP flavor structure, from Refs [24, 25]. The last column corresponds to the bound on the gluon excitation in FHQT in **case B** as described in the text.

In general, there will be a similar situation for other values of N as long as these are

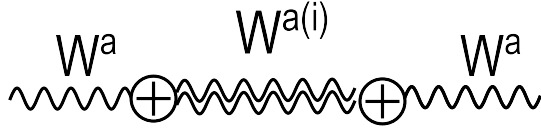


Figure 10. Diagrams contributing to S and T through the exchange of the excited states of the $SU(2)_L \times U(1)_L$ gauge bosons. The circled crosses denote the mixing with the zero modes.

small enough to be away from the continuum limit. Also, here we are studying FHQT with a very large cutoff, of the order of the Planck scale. However, it is worth studying flavor models and their bounds with smaller UV cutoffs. We leave these studies for future work.

5 Electroweak Precision Constraints

Another important set of bounds comes from precision electroweak measurements. Particularly binding are the S and T parameters defined as

$$S = 16\pi (\Pi'_{33}(0) - \Pi'_{3Q}(0)) \quad (5.1)$$

and

$$\alpha T = \frac{4}{v_{EW}^2} (\Pi_{11}(0) - \Pi_{33}(0)) \quad (5.2)$$

In order to compute S and T , we first need to choose an electroweak sector to propagate in the quiver. The minimal choice is to take $G_j = SU(2)_L \times U(1)_Y$ for all values of j . In AdS_5 this would be equivalent to have the SM gauge fields propagate in the bulk. This is an unacceptable choice in AdS_5 models since it results in too large isospin violation and contributions to the T parameter. As we will see below, this is not the case for the coarse FHQT we study here, $N = 4$. So we will study the electroweak sector of the SM propagating in the quiver.

Although in most extensions of the SM contributions to S and T start arising at loop level, in FHQT -just as in AdS_5 models- there are effects arising already at tree level. These are driven by the mixing of the low-lying gauge bosons W^\pm and Z with their excited states through the Higgs VEV. The mixing effect leads to contributions to oblique parameters through the exchange of excited states, as shown in Figure 10. However, these are not the largest contributions to S and T . There are additional contributions arising from the universal shifts in the gauge couplings of light fermions which result from the mixing, as illustrated in Figure 11. The contributions to the S parameter arising from diagrams like the ones in Figure 10 are suppressed by a factor of v^4/M_1^4 and will not be the leading source of S , which receives much larger contributions from the universal shift of gauge couplings that result from the diagrams of Figure 11. On the other hand, the contributions of the exchange diagrams of Figure 10 to T cannot be neglected.

As mentioned in the previous section, the choice of fermion localization we called **case A**, which has negligible flavor violation, will result in larger contributions to S and T . This increase, with respect to **case B**, comes from the fact that the universal shifts in gauge

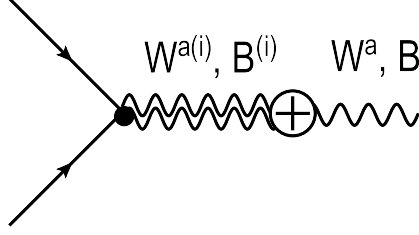


Figure 11. Universal tree-level renormalization of the $SU(2)_L \times U(1)_Y$ gauge couplings to fermions. The circled crosses denote the mixing of the excited state with the zero-mode gauge bosons.

couplings induced by the diagrams of Figure 11 are enhanced when the light left-handed fermions are localized close to the N site. We will then concentrate in the result for **case B**, where light fermions are localized closer to the UV site. For this localization the exchange diagrams of Figure 11 result in

$$T_e \simeq 0.05 \times \left(\frac{3 \text{ TeV}}{M_1} \right)^2, \quad (5.3)$$

where M_1 is the mass of the first excited gauge boson state. The universal part of the vertex corrections illustrated in Figure 11 can be absorbed to a redefinition of the electroweak gauge fields, which result in additional contributions to S and T , analogously to the AdS₅ case [27]. The universal vertex corrections resulting from the mixing of electroweak gauge bosons with their excited states can be absorbed by the field redefinitions

$$\begin{aligned} W^\pm &\rightarrow W^\pm(1 - g^2\delta) \\ W^3 &\rightarrow W^3(1 - g^2\delta) + B g g' \delta \\ B &\rightarrow B(1 - g'^2\delta) + W^3 g g' \delta, \end{aligned} \quad (5.4)$$

with

$$\delta = -\frac{g_{01} g}{4} \left(\frac{v}{M_1} \right)^2 f_{N,0} f_{N,1}. \quad (5.5)$$

In (5.5) g_{01} is the coupling of the first excited state of the gauge bosons to the zero-mode fermions, given by (4.3). These shifts restore the gauge couplings to their SM values at tree level, but result in new contributions to oblique parameters:

$$\begin{aligned} S_v &= 32\pi\delta \\ T_v &= \frac{8\pi}{\cos^2\theta_W} \delta. \end{aligned} \quad (5.6)$$

(For comparison, the **case A** localization results in vertex contributions to S and T that are roughly a factor of four larger than the ones in (5.6).) Adding the exchange and vertex contributions we obtain, for the **case B** localization

$$\begin{aligned} S &\simeq 0.17 \times \left(\frac{3 \text{ TeV}}{M_1} \right)^2 \\ T &\simeq 0.16 \times \left(\frac{3 \text{ TeV}}{M_1} \right)^2. \end{aligned} \quad (5.7)$$

The experimental fit to oblique parameters with $m_t = 173$ GeV and $m_h = 126$ GeV as reference values, results in [28] $S^{\text{exp.}} = 0.03 \pm 0.10$ and $T^{\text{exp.}} = 0.05 \pm 0.12$. Thus, we see that a mass scale of $M_1 = 3$ TeV is well within the 95% C.L. bounds. Then, this is the bound on the excited gauge boson masses that passes all flavor and electroweak tests.

Additional contributions to S and T come from loops, particularly of excited fermion states. We will study them elsewhere. There will also be contributions from the link field sector [17]. These are sub-leading compared to the ones shown above.

6 Conclusions and Outlook

We have presented a class of theories in four dimensions, FHQT, which have interesting properties for model building at the TeV scale. Although these theories can be obtained from the deconstruction of AdS₅ models, they have distinct properties and phenomenology. They can accommodate large hierarchies, both between the IR and UV scales, as well as in the fermion spectrum, just as AdS₅ models. However, as shown in Section 4, they have less flavor violation at tree level when compared with typical AdS₅ models, even when fermion masses are entirely obtained from localization in the quiver and governed by order one parameters. As a result, flavor bounds allow the IR mass scale to be lower than in 5D models, typically as low as 3 TeV, without the introduction of ad-hoc flavor symmetries. We also showed in Section 5 that the same localization models that have this flavor bound, called **case B** in Section 4, pass electroweak precision constraints for the same value of the excited state mass scale, even without the extension of the electroweak gauge sector to provide custodial protection. This is quite different from the AdS₅, where the bulk electroweak gauge sector must be extended beyond the SM in order to avoid large contributions to the T parameter [27]. Thus, despite being related to AdS₅ models by having them as their continuum limit, FHQT for small values of N have distinct phenomenological features. In particular, it is possible to build models of EWSB and fermion masses with them that pass electroweak precision and flavor bounds while still having their IR scale naturally close to the TeV scale.

There are several avenues to explore further. First, the Higgs sector must be introduced dynamically so as to naturally result in a light Higgs when compared with the IR scale of a few TeV. A way to achieve this “little hierarchy” is for the Higgs to be a pNGB. This is very similar to the composite Higgs models that are built in AdS₅ [12, 18], and can be essentially regarded as their (coarse) deconstruction [17]. Specific realizations of this idea in the context of FHQT will be presented elsewhere [11].

The phenomenology of models of EWSB built using FHQT should be explored at the LHC, since it is quantitatively different from that of AdS₅ models. For the case when color propagates in the quiver, which was used as a way to obtain the strongest bounds from flavor physics, production and decay of the first color-octet resonance at the LHC is qualitatively similar to those of the KK gluon in AdS₅. However, its couplings to zero-mode fermions are quite different, as illustrated in Figures 4 to 9. For a fixed value of the UV

cutoff, these couplings depend on the number of sites N . It will be necessary to do a detailed study of this dependence in order to search for the resonances in specific FHQT. On the other hand, in general it is not necessary for color to propagate in the quiver. The minimal models using FHQT will only contain the electroweak sector. Thus the phenomenology of these weakly-coupled massive gauge bosons should be considered separately. Finally, the lepton sector of FQHT must be studied to complete models of fermion masses, as well as to study the complementary phenomenology with leptons in the final state at the LHC.

As the LHC increases its reach in the search for physics beyond the SM, building models of the TeV scale with FHQT for EWSB and the Higgs sector, fermion masses and other questions typical of this energy scale, will provide a rich phenomenology beyond that of AdS_5 models. In particular, FHQT for small number of sites N will give a more complete picture of these class of theories which includes AdS_5 as a limit. Ultimately, and just as is the case for AdS_5 models, the hope is that FHQT are a description of the TeV scale that will guide us through its phenomenology to a deeper understanding of the underlying dynamics of that scale.

Acknowledgments: The authors acknowledge the support of the State of São Paulo Research Foundation (FAPESP), and the Brazilian National Counsel for Technological and Scientific Development (CNPq).

References

- [1] K. Nakamura *et al.* [Particle Data Group Collaboration], *Review of particle physics*, J. Phys. G **G37**, 075021 (2010).
- [2] G. Aad *et al.* [ATLAS Collaboration], *Observation of a new particle in the search for the Standard Model Higgs boson with the ATLAS detector at the LHC*, Phys. Lett. B **716**, 1 (2012) [arXiv:1207.7214 [hep-ex]];
S. Chatrchyan *et al.* [CMS Collaboration], *Observation of a new boson at a mass of 125 GeV with the CMS experiment at the LHC*, Phys. Lett. B **716**, 30 (2012) [arXiv:1207.7235 [hep-ex]].
- [3] For review see H. Baer and X. Tata, *Weak scale supersymmetry: From superfields to scattering events*, Cambridge, UK: Univ. Pr. (2006) 537 p
- [4] C. T. Hill and E. H. Simmons, *Strong dynamics and electroweak symmetry breaking*, Phys. Rept. **381**, 235 (2003), [Erratum-ibid. **390**, 553 (2004)], [arXiv:hep-ph/0203079].
- [5] L. Randall and R. Sundrum, *A Large mass hierarchy from a small extra dimension*, Phys. Rev. Lett. **83**, 3370 (1999) [hep-ph/9905221].
- [6] Y. Grossman and M. Neubert, *Neutrino masses and mixings in non-factorizable geometry*, Phys. Lett. B **474**, 361 (2000), [arXiv:hep-ph/9912408];
S. Chang, J. Hisano, H. Nakano, N. Okada and M. Yamaguchi, *Bulk standard model in the Randall-Sundrum background*, Phys. Rev. D **62**, 084025 (2000), [arXiv:hep-ph/9912498];
H. Davoudiasl, J. L. Hewett and T. G. Rizzo, *Experimental probes of localized gravity: On and off the wall*, Phys. Rev. D **63**, 075004 (2001), [arXiv:hep-ph/0006041].
- [7] T. Gherghetta and A. Pomarol, *Bulk fields and supersymmetry in a slice of AdS*, Nucl. Phys. B **586**, 141 (2000) [hep-ph/0003129].

- [8] C. Csaki, A. Falkowski and A. Weiler, *The Flavor of the Composite Pseudo-Goldstone Higgs*, JHEP **0809**, 008 (2008) [arXiv:0804.1954 [hep-ph]].
- [9] N. Arkani-Hamed, A. G. Cohen and H. Georgi, *(De)constructing dimensions*, Phys. Rev. Lett. **86**, 4757 (2001) [arXiv:hep-th/0104005];
C. T. Hill, S. Pokorski and J. Wang, *Gauge invariant effective Lagrangian for Kaluza-Klein modes*, Phys. Rev. D **64**, 105005 (2001) [arXiv:hep-th/0104035].
- [10] R. Contino, T. Kramer, M. Son and R. Sundrum, *Warped/composite phenomenology simplified*, JHEP **0705**, 074 (2007) [hep-ph/0612180].
- [11] G. Burdman, N. Fonseca and L. Lima, in preparation.
- [12] R. Contino, Y. Nomura and A. Pomarol, *Higgs as a holographic pseudo-Goldstone boson*, Nucl. Phys. B **671**, 148 (2003), [arXiv:hep-ph/0306259];
K. Agashe, R. Contino and A. Pomarol, *The minimal composite Higgs model*, Nucl. Phys. B **719**, 165 (2005), [arXiv:hep-ph/0412089].
- [13] R. S. Chivukula, B. Coleppa, S. Di Chiara, E. H. Simmons, H. -J. He, M. Kurachi and M. Tanabashi, *A Three Site Higgsless Model*, Phys. Rev. D **74**, 075011 (2006) [hep-ph/0607124].
- [14] T. Abe, R. S. Chivukula, E. H. Simmons and M. Tanabashi, *The Flavor Structure of the Three-Site Higgsless Model*, Phys. Rev. D **85**, 035015 (2012) [arXiv:1109.5856 [hep-ph]].
- [15] M. Redi and A. Weiler, *Flavor and CP Invariant Composite Higgs Models*, JHEP **1111**, 108 (2011) [arXiv:1106.6357 [hep-ph]].
- [16] S. De Curtis, M. Redi and A. Tesi, *The 4D Composite Higgs*, JHEP **1204**, 042 (2012) [arXiv:1110.1613 [hep-ph]].
- [17] G. Panico and A. Wulzer, *The Discrete Composite Higgs Model*, JHEP **1109**, 135 (2011) [arXiv:1106.2719 [hep-ph]].
- [18] D. Marzocca, M. Serone and J. Shu, *General Composite Higgs Models*, JHEP **1208**, 013 (2012) [arXiv:1205.0770 [hep-ph]].
- [19] H. Abe, T. Kobayashi, N. Maru and K. Yoshioka, *Field localization in warped gauge theories*, Phys. Rev. D **67**, 045019 (2003) [hep-ph/0205344].
- [20] A. Falkowski, H. D. Kim, *Running of gauge couplings in AdS(5) via deconstruction*, JHEP **0208**, 052 (2002). [hep-ph/0208058];
L. Randall, Y. Shadmi, N. Weiner, *Deconstruction and gauge theories in AdS(5)*, JHEP **0301**, 055 (2003). [hep-th/0208120];
- [21] J. de Blas, A. Falkowski, M. Perez-Victoria, S. Pokorski, *Tools for deconstructing gauge theories in AdS(5)*, JHEP **0608**, 061 (2006). [hep-th/0605150].
- [22] Y. Bai, G. Burdman, C. T. Hill, *Topological Interactions in Warped Extra Dimensions*, JHEP **1002**, 049 (2010). [arXiv:0911.1358 [hep-ph]].
- [23] C. Csaki, A. Falkowski, A. Weiler, *The Flavor of the Composite Pseudo-Goldstone Higgs*, JHEP **0809**, 008 (2008). [arXiv:0804.1954 [hep-ph]].
- [24] M. Bona *et al.* [UTfit Collaboration], *Model-independent constraints on $\Delta F=2$ operators and the scale of new physics*, JHEP **0803**, 049 (2008) [arXiv:0707.0636 [hep-ph]].
- [25] V. Bertone, N. Carrasco, M. Ciuchini, P. Dimopoulos, R. Frezzotti, V. Gimenez, V. Lubicz

and G. Martinelli *et al.*, *Kaon Mixing Beyond the SM from $N_f=2$ tmQCD and model independent constraints from the UTA*, arXiv:1207.1287 [hep-lat].

- [26] F. del Aguila, J. A. Aguilar-Saavedra, B. C. Allanach, J. Alwall, Y. .Andreev, D. Aristizabal Sierra, A. Bartl and M. Beccaria *et al.*, *Collider aspects of flavour physics at high Q* , Eur. Phys. J. C **57**, 183 (2008), [arXiv:0801.1800 [hep-ph]].
- [27] K. Agashe, A. Delgado, M. J. May and R. Sundrum, *RS1, custodial isospin and precision tests*, JHEP **0308**, 050 (2003) [hep-ph/0308036].
- [28] The Gfitter Collaboration, M. Baak, M. Goebel, J. Haller, A. Hoecker, D. Kennedy, R. Kogler, K. Moenig and M. Schott *et al.*, *The Electroweak Fit of the Standard Model after the Discovery of a New Boson at the LHC*, arXiv:1209.2716 [hep-ph].